Entropy of point defects calculated within periodic boundary conditions

E. Rauls* and Th. Frauenheim
Theoretical Physics, Physics Department, Faculty of Science, University of Paderborn, Warburger Strasse 100, D-33098 Paderborn, Germany

(Received 30 September 2003; revised manuscript received 22 December 2003; published 30 April 2004)

A possibility to calculate both the entropies of formation and migration of point defects in semiconductors is presented. Knowledge of the entropic contributions is especially important for the correct description of high-temperature processes like growth or annealing. Using the self-consistent charge density-functional based tight-binding method (SCC-DFTB) we have calculated the predominant part of the entropy, resulting from lattice vibrations. Strong finite-size effects have been observed while investigating the formation entropies of isolated vacancies in diamond and silicon. We demonstrate how these problems can be overcome with the help of linear elasticity theory.

DOI: 10.1103/PhysRevB.69.155213 PACS number(s): 71.15.Pd, 65.40.Gr, 81.40.Jj

I. INTRODUCTION

In common computer simulations of point defects in semiconductors, the total energy obtained from quantum-mechanical calculations at a temperature $T=0$ K is used for calculating the formation energies or the migration energy barriers in diffusion processes, respectively. It would, admittedly, be thermodynamically correct to consider also the temperature-dependent contributions of entropy. In the past, calculations were computationally too demanding to take this term (fully) into account. Its neglect can often be justified by the similarity of the compared structures, which suggests comparable entropic contributions and thus only small entropy differences. In some cases, though, it is important to consider the entropic corrections to the total energy. For the correct description of high-temperature processes, i.e., defect migration processes during the postimplantation annealing phase, entropic corrections can become quite large, since a substantial rearrangement of the bonding situation around the defects can occur. This can result in strong changes in the local vibrational modes linked to the defect, and the elevated temperatures amplify this effect, so that the entropic contribution $-T\cdot\Delta S$ is no longer negligible. In our previous investigations of annealing processes in silicon carbide (SiC), we have found that activation energies in the range of ≈ 5 eV for vacancy- and antisite-related processes are lowered by up to 1.3 eV at common annealing temperatures ($T=1800$ K), if one considers the entropic contributions.[1] Furthermore, knowing the formation entropy of a defect allows the calculation of its concentration. In case of migration processes, it permits the calculation of diffusivities that can be directly compared to experimental data (see also Ref. 1).

In this work, we present the theoretical background of these calculations, and further considerations about the calculation of formation entropies within supercell methods. In contrast to the case of activation energies, the number of atoms can be different in the structures that have to be compared in order to calculate the formation entropy. Due to the long range character of the entropy and additional finite-size effects, i.e., a strong dependence of the results on the size of the supercell used, elasticity theory has to be used in combination with quantum-mechanical calculations.

We describe how a systematic study of the influence of entropic contributions is possible within common supercell methods. As it is still a rather time consuming task, we have used the computationally efficient self-consistent charge–density-functional-based tight-binding (SCC-DFTB) method[2] for our investigations.

This paper is organized as follows. Section II gives a short description of the computational method and the theoretical background of how the vibrational entropy can be obtained. In Sec. III, we calculate the specific heat for silicon, diamond, and SiC, and validate the use of our approximate method with first-principle calculations and experimental data. In Sec. IV, we derive the correction terms to the formation entropy from elasticity theory at the example of isolated vacancies. The results for the vacancy in diamond and in silicon are discussed in Sec. V. Finally, in Sec. VI, we briefly summarize the influence of the vibrational entropy on activation energies for migration processes.

II. LATTICE VIBRATIONS AND FREE ENERGIES

For the calculation of formation energies of defects or activation energies of migration processes, the energies of different structures have to be compared. This is most often done by simply comparing the total energies E_{tot} obtained from, e.g., supercell calculations. Spoken thermodynamically, however, the crystal (with the defect) is a great canonical ensemble, and it would be thermodynamically correct to compare the Gibbs free enthalpies

$$G=U-T\cdot S+p\cdot V+\sum_i \mu_i N_i \tag{1}$$

of the structures. Here, U is the internal energy

$$U=E_{\mathrm{tot}}+U_{\mathrm{vib}}, \tag{2}$$

where the first term, the static part, is the total energy E_{tot}, as obtained from quantum-mechanical calculations (as usual at $T=0$ K). The term U_{vib} is caused by lattice vibrations. The second term in Eq. (1) accounts for the temperature dependence and the entropic contributions. The term $p\cdot V$, i.e., the dependence of G on pressure and volume is usually ne-

glected, since most often systems are treated for constant pressure and/or volume conditions. The last term accounts for the change in particle number N_i with the chemical potential μ_i.

Due to the immense computational effort needed to calculate the entropy S and the vibrational part of U, these terms are usually neglected. In many cases, this is justified by the similarity of the structures that are compared, so that the change in entropy ΔS is, indeed, very small. In some cases however, as, e.g., strong rearrangements of the lattice, it is important to consider the term $T \cdot S$ explicitly, in particular at high temperatures. In this work, we present a way to calculate U and S and obtain, thus, the free energy of formation of a defect and the free activation energy for migration processes of defects.

The entropy S consists of the configurational, the electron-hole pair, and the vibrational entropy (cf. Refs. 3–5). The configurational term is given by the number of possible configurations in which the defect can exist. The second term is usually negligibly small[4] and shall also not be discussed further. The prevailing contributions to the entropy arise from the lattice vibrations.

Assuming a Planck distribution of harmonic oscillators, U_{vib} can be written as

$$U_{\mathrm{vib}} = \sum_{i=1}^{3N} \left\{ \frac{\hbar \omega_i}{\exp(\hbar \omega_i / k_B T) - 1} + \frac{1}{2} \hbar \omega_i \right\}, \tag{3}$$

(compare, e.g., Ref. 6). Here, ω_i are the eigenfrequencies obtained from the calculation of the vibrational spectrum of the defect. T is the temperature.

From this equation, the entropy S can be calculated according to the thermodynamic relation

$$\left(\frac{\partial S}{\partial U} \right)_{\mathrm{V,N}} = \frac{1}{\left(\frac{\partial U}{\partial S} \right)_{\mathrm{V,N}}} = \frac{1}{T(U,V,N)}, \tag{4}$$

assuming constant volume V (as already stated above) and constant number of particles N.

With Eqs. (3) and (4), the expression for the vibrational entropy S_{vib} becomes

$$S_{\mathrm{vib}} = k_B \sum_{i=1}^{3N} \left\{ \frac{\hbar \omega_i}{k_B T} \left[\exp\left(\frac{\hbar \omega_i}{k_B T} \right) - 1 \right]^{-1} - \ln\left[1 - \exp\left(\frac{-\hbar \omega_i}{k_B T} \right) \right] \right\}. \tag{5}$$

Although this expression can be derived from simple thermodynamics, the entropy is not easily accessible, neither experimentally nor theoretically. The calculation of the local vibrational frequencies ω_i of the defect structure, which determine U_{vib} and S_{vib}, is a very time consuming task. They can be calculated from the dynamical (Hessian) matrix

$$D_{ij} = \frac{1}{\sqrt{m_k m_l}} \frac{\partial^2 E}{\partial r_{ik} \partial r_{jl}}, \tag{6}$$

which is defined by the second derivatives of the energy having the eigenvalues ω_i^2. The most common way to construct the Hessian matrix is to displace each atom (in the defective region) by $\pm \Delta r_i$ in six directions. Based on the finite differences in the forces in these slightly different geometries, the Hessian matrix can easily be constructed. Its subsequent diagonalization yields the desired frequencies.

Due to the high computational demands, *ab initio* methods are often limited to the use of small supercells and the calculation of the local vibrational modes for small defective regions only. Furthermore, the diagonalization of large matrices can make numerical problems. A common approach is, therefore, to use the local harmonic approximation (LHA) for the nearest and next-nearest neighbors of the defect, in which the atoms are treated as independent oscillators (see, e.g., Refs. 7,8). The advantage is that the diagonalization of large matrices in order to obtain the frequencies is circumvented. As shown, e.g., in Ref. 9, this approximation yields in some cases rather poor results.

Other, more approximate methods often do not reach the necessary accuracy in the description of the forces, which is required for the calculation of vibrational frequencies. A very efficient method which at the same time in its accuracy is close to *ab initio* methods is the SCC-DFTB method.[2] In this work, we have used the SCC-DFTB method for the calculation of the relaxed geometries, the migration paths, and the vibrational spectra of all defects discussed. The vibrational frequencies are obtained from the calculation and diagonalization of the complete dynamical matrix for the supercells used. Throughout this work, a minimal basis set and the Γ-point approximation were used. (A detailed discussion of the accuracy of this approach in comparison to common *ab initio* approaches can be found in Ref. 1.) If not otherwise stated, defects were modeled using cubic $(3\times3\times3)$ supercells containing 216 atoms. Since the potential-energy surface of silicon is extremely flat, we have checked convergence by repeating the same calculations for the isolated vacancy within the $(4\times4\times4)$ supercell containing 512 atoms.

By comparing our results (for a perfect crystal) with available data of first-principle methods AIMPRO (Ref. 10) and FHI,[11] we will show in the following that the accuracy of the calculated vibrational frequencies is sufficient to obtain the derived quantities, such as the heat capacity and the entropy, with deviations between the different methods of substantially less than 0.1 eV.

III. RESULTS

Because of the computational problems described in the preceding section, there are only few data available in the literature. While there exist several theoretical papers for the isolated vacancy in silicon (compare Secs. III C and III D) and in copper, only sporadic work has focussed on vacancies in other materials. Also experimentally, almost no data that could be used for comparison with our theoretical results is available. Nevertheless, experimental values are known for the heat capacity C_{v} which can be derived from U_{vib}.

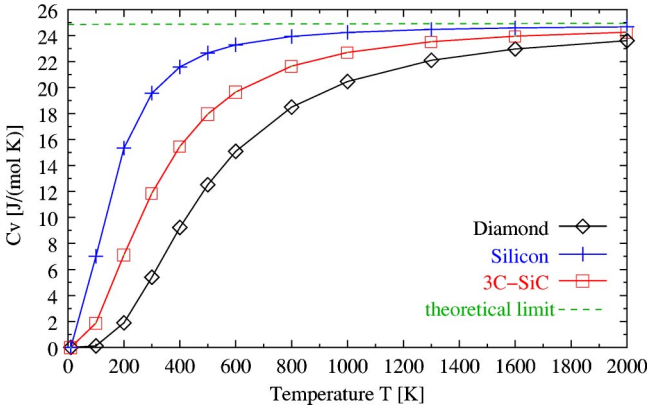

FIG. 1. (Color online) Calculated temperature dependence of C_v for diamond, silicon, and 3C-SiC. The dashed line denotes the theoretical limit of $3Nk_B$, which is reached by any solid for temperatures above the material dependent Debye temperature Θ_D.

A. Heat capacity of diamond, silicon, and SiC

The heat capacity C_v at constant volume can be calculated from Eq. (3) as the derivative of U_{vib} with respect to T:

$$C_v = \left(\frac{\partial U_{vib}}{\partial T}\right)_V = \sum_{i=1}^{3N} \left\{ k_B \left(\frac{\hbar\omega_i}{k_B T}\right) \frac{\exp\left(\frac{\hbar\omega_i}{k_B T}\right)}{\left[\exp\left(\frac{\hbar\omega_i}{k_B T}\right) - 1\right]^2} \right\}. \tag{7}$$

For high temperatures, C_v approaches $3Nk_B$, in agreement with the rule of Dulong and Petit.[6]

In Fig. 1, the calculated C_v is plotted for diamond, silicon, and 3C-SiC in a temperature range between 0 and 2000 K. The shape and the asymptotic behavior of the curves and the differences between the materials, as, e.g., the Debye temperature Θ_D [Si, 741 K (expt, 650 K); C, 2021 K (expt, 2230 K); SiC, 1456 K (expt, 1600 K)], are described correctly.

Calculating now the (mass-dependent) specific heat c, we obtain $c = 0.450$ J/(g K) for diamond, $c = 0.699$ J/(g K) for silicon, and 0.563 J/(g K) for 3C-SiC, which agrees reasonably with the experimental values of 0.502, 0.703, and 0.678 J/(g K) as given in Ref. 12 for $T = 300$ K. The whole curves are shown in Fig. 2.

Experimental results and the temperature dependence as predicted by the Einstein model are, thus, described qualitatively correct by the vibrational spectrum calculated numerically within SCC-DFTB. From the experimental point of view, this gives the validation for using this method for the calculation of the vibrational parts of the internal energy and the entropy. Before turning to the investigation of defects, we first mark the expectable accuracy of our results from the theoretical side also.

B. Absolute entropy in different methods

Following the procedure described above, the vibrational entropy and the internal energy of vibration can be calculated. Figure 3 shows the temperature dependence of the absolute entropy, scaled by the number of atoms in the supercell used. For comparison to our data, we have also calculated U_{vib} and S_{vib} from the vibrational frequencies obtained by AIMPRO (Ref. 13) and FHI (Ref. 14) calculations of 64-atom supercells. The vibrational spectrum calculated with the FHI-code reproduces the experimental properties, i.e., the phonon band gap, best, and is therefore used as a reference curve. The slope of the AIMPRO curve is slightly too large, while that of the SCC-DFTB curve, calculated in the equal sized 64-atom supercell, is by about the same amount too flat. However, the SCC-DFTB calculation in the 216-atom supercell reproduces the FHI curve nearly exactly. The internal energy U does not show strong deviations between the different methods, except for the very low-temperature range. This range is, actually, not described correctly in the underlying theoretical model, since, here, the Debye model would have to be used instead (cf. Ref. 6). For applications, this low-temperature range is, however, not of high relevance, because the approximation $\Delta G \approx \Delta E_{tot}$ becomes valid.

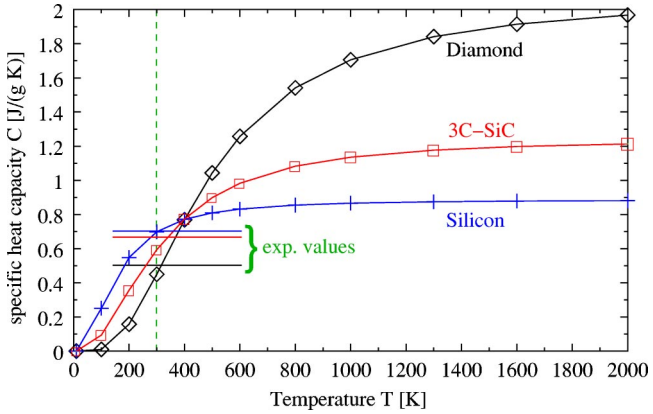

FIG. 2. (Color online) Calculated specific-heat capacity for diamond, silicon, and 3C-SiC compared to experimental values at $T = 300$ K.

Since the errors in the description of frequencies concern any structure calculated within one method in the same way, the variations of the quantity of interest between the different

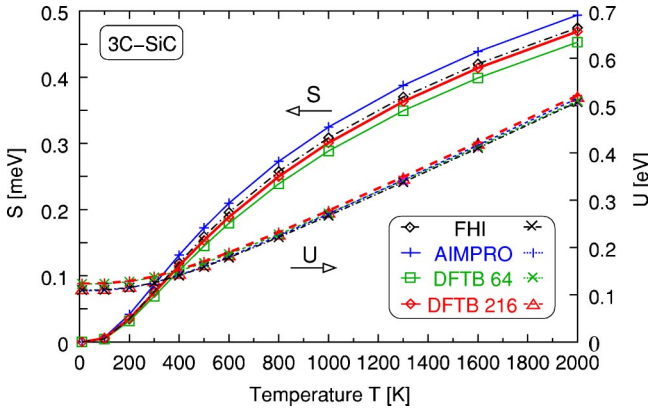

FIG. 3. (Color online) The perfect SiC bulk: Temperature dependence of the absolute entropy S (*left ordinate*) and the internal energy U (*right ordinate*), scaled by the number of atoms in the supercell used.

methods, i.e., the entropy difference ΔS between two structures, can be expected to be even smaller.

C. Formation entropy

The calculation of formation entropies of defects is by far more complicated and not as straightforward as the calculation of formation energies. First, the entropies of the defective crystal and of the perfect crystal have to be calculated as described in Sec. II. Analogous to the formation energy, the formation entropy is then calculated as the difference

$$S_{\text{form}} = S_{\text{defect}} - S_{\text{perfect}}, \tag{8}$$

with additionally invoking an appropriate scaling factor to account for the different numbers of atoms in the two structures. To calculate, e.g., the formation entropy of an isolated vacancy, the dynamical matrices have to be calculated both for the supercell with the vacancy and for the perfect supercell. The absolute entropies can then be calculated as described in Sec. II. To correct the different numbers of atoms in the two cells, the results for the perfect lattice have to be multiplied by $(N-1)/N$, where N is the number of atoms in the perfect lattice cluster.

Because of the artificial periodic images caused by the finite supercells used, the treatment of these small differences is affected by strong finite-size effects. This is, e.g., well known from the case of electrostatic Coulombic interactions, where the evaluation of the Coulombic integrals in some cases necessitates the definition of a cutoff radius to avoid artificial interactions with the periodic images.[15] As already described in Refs. 9,17, we have found a strong dependence on the cluster and supercell size. The reasons for this and how to correct for it is discussed in the following at the example of an isolated vacancy in diamond and in silicon.

The periodic images of a defect strongly influence the formation entropy which is an unavoidable artifact due to the supercell approach. This is certainly also true for formation energies, but the effect is by far not as large as for the long-range character of formation entropies. Because of the change in the *collective* vibrational properties of the defect, the entropy is to a large extent stored in the material outside the defect region. It has been found that, in order to simulate the behavior of a defect in a nearly infinite crystal, modeling is done best by using an *embedded cluster scheme*, i.e., dividing the fully relaxed supercell with the defect into a region around the defect, the ''cluster,'' in which all atoms are treated dynamically, and an outer region in which the atoms are treated as static,[9,17,18] compare Fig. 4.

Calculations with several different methods for the modeling of the vibrational behavior have shown that the cluster size must be essentially smaller than the size of the supercell.[9,17] On the other hand the cluster size must be large enough to provide a correct description of the defect. In Ref. 18, the authors used cells of about 5000 atoms to model an isolated vacancy in copper, whereof only about 100 to 500 atoms were then included in the calculation of the vibrational spectra. In Ref. 9, cells of up to 16 384 atoms were used, treating up to 1289 atoms dynamically. In these calculations Born-Mayer and Morse potentials were used for the entropy calculations.

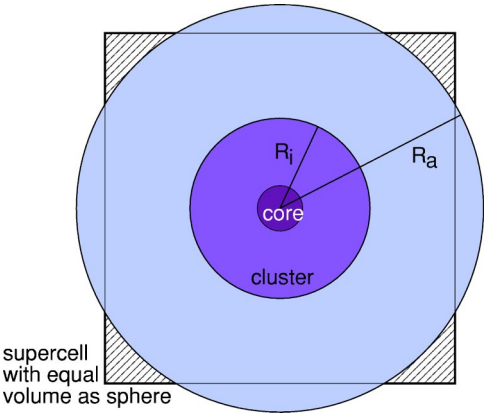

FIG. 4. (Color online) The supercell used for modeling the defect is divided into a spherical *cluster* with radius R_i (containing the defect core), which is treated dynamically within the atomistic calculation, and an outer sphere with radius R_a, which is treated by linear elasticity theory and is supposed to have the same volume as the supercell.

Such large supercells are, of course, far beyond the supercell sizes that can be treated within atomistic calculations, especially since the diagonalization of the dynamical matrix does not only take a very long time but is also associated with numerical problems.

Nevertheless, based on the corrections proposed by these authors, entropy calculations can also be performed in our smaller supercells containing 216 atoms. The comparison with the calculation in a supercell with 512 atoms for the vacancy in silicon shows that a consistent picture can be obtained. Due to the long-range character of the entropy, however, a large part of it is stored in the region outside the cluster, which is not included in the atomistic calculation. This elastic part has, therefore, to be calculated separately and added to the values obtained by the atomistic calculation. It can be divided into two ''correction terms'' that can be derived within linear elasticity theory, compare the Appendix. As described in detail in, e.g., Ref. 19, the R dependence of the elastic constants [cf. Eqs. (A2) and (A5)] transmits to the entropy, such that the entropy stored outside a sphere with radius R is proportional to $1/R^3$. Since the number N of atoms is proportional to R^3, the correction

$$\Delta S_1 = \frac{k}{N} \tag{9}$$

is obtained for the formation entropy with a constant k depending on the material.[18]

Following the procedure proposed by Hatcher *et al.*,[18] the entropy values obtained like this require a further correction ΔS_2 that accounts for the image forces introduced by the periodic images of the defect and the entropy stored in the up to now neglected region of the crystal outside the defect cluster. The size of this correction can be calculated from the free energy,[19] resulting in

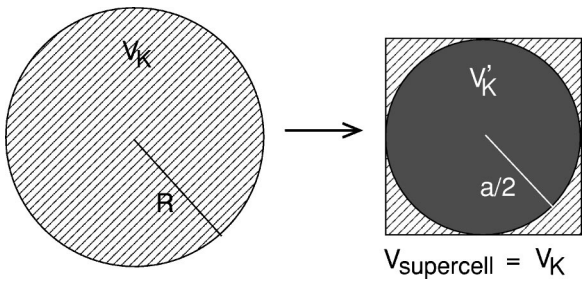

FIG. 5. Sphere inscribed in a supercell.

$$\Delta S_2 = B\alpha \Delta V^{\text{image}}, \tag{10}$$

with the bulk modulus K, the thermal expansion coefficient α, and the volume change ΔV^{image} due to image forces. This term can be split into two parts as motivated in the following. The idea for this finite-size correction comes again from linear elasticity theory: at the boundary of the supercell—for simplicity we regard the boundary of an outer sphere of radius R_a and assume isotropic dilatation (compare Fig. 4)—the inevitably vanishing displacements of the atoms introduce a volume change

$$\Delta V = -\left(\frac{R_i}{R_a}\right)^3 \Delta V^{\text{tot}} \approx -\left(\frac{N}{N_Z}\right)\Delta V^{\text{tot}} \tag{11}$$

at the inner sphere of radius R_i (which contains the dynamically treated cluster in our calculations) (Refs. 18,19). ΔV^{tot} is the relaxation volume of the defect in an infinitely extended crystal.

In reality however, we always have a finite crystal terminated by the crystal surfaces. In supercell calculations, the simulated region is limited by the supercell boundaries. The volume change introduced by the defect is influenced by these constraints, and as derived in the Appendix, the fraction $\frac{2}{3}[(1-2\nu)/(1-\nu)]$ of the volume change ΔV^{tot} is the dilatation part that is caused by image forces (with the Poisson ratio ν).

For these considerations a sphere of radius R was used, but the atomistic calculations were as usual performed in cubic supercells with the same volume and edge length a. Due to the influence of neighboring cells, the postulation of isotropy may not apply to the marginal regions of the supercell. We, therefore, have to go over to a sphere with radius $a/2$ that is inscribed in the supercell, as denoted in Fig. 5. Since the ratio of these volumina is

$$\frac{V_K'}{V_K} = \frac{V_K'}{V_{\text{supercell}}} = \frac{\frac{4\pi}{3}\left(\frac{a}{2}\right)^3}{a^3} = \frac{\pi}{6}, \tag{12}$$

the smaller volume $(\pi/6)\cdot\Delta V_d$ has to be used in Eq. (10).

Expressing the total volume change by the volume change of the defect core

$$\frac{\Delta V_{\text{tot}}}{\Delta V_{\text{core}}} \approx \frac{R_a^3}{r_{\text{core}}^3} \approx \frac{N_Z}{n_{\text{core}}}, \tag{13}$$

TABLE I. Data used for the calculation of the entropy of formation of an isolated vacancy in diamond and silicon. The bulk modulus B has been calculated within SCC-DFTB. Experimental values (Poisson ratio ν, thermal expansion coefficient α) were taken from Ref. 16.

	Diamond	Silicon
B	536 GPa	100 GPa
ν	0.1	0.29
α	7.1×10^{-6} K^{-1}	2.6×10^{-6} K^{-1}
N_Z	216	216, 512
n_{core}	17	17
ΔV_{core}	-1.330 Å^3	-21.37 Å^3
V_{tot}	1226 Å^3	4310 Å^3 (216)
		10240 Å^3 (512)

and inserting Eqs. (11) and (A17) into Eq. (10), the final expression for the correction of the formation entropy becomes

$$\Delta S = \frac{k}{N} + B\alpha\left(\frac{2}{3}\frac{(1-2\nu)}{(1-\nu)}\frac{\pi}{6} - \frac{N}{N_Z}\right)\frac{N_Z}{n_{\text{core}}}\Delta V^{\text{core}}. \tag{14}$$

Due to the numerous assumptions and approximations, i.e., spherical symmetry of the defect core, the cluster and the complete supercell in order to use the macroscopic continuum theory for a furthermore rather small number of atoms as can be treated in our supercell calculations, results can only be expected to be of qualitative accuracy. Nevertheless, the results for isolated vacancies in diamond and silicon presented in the following section are quite encouraging.

D. The vacancy in diamond and silicon

The procedure described above has been applied to the calculation of the formation entropy of isolated vacancies in diamond and silicon, using the data given in Table I. A temperature of $T=2000$ K has been chosen, where the high-temperature approximation is valid and the formation entropy becomes temperature independent (compare Fig. 1 and the discussion of the Debye temperatures in Sec. III A).

The results of these calculations are shown in Fig. 6. In the upper diagram, the values of S_{form} of the vacancy in diamond obtained from the calculation without any corrections are plotted over the relative cluster size N/N_Z (black diamonds), the corrected values are plotted in gray. The solid line has been fitted to these values, so that the desired value for $N=N_Z$ can be extrapolated, resulting in $S_{\text{form}}=2.85k_B$. Variations of the corrected values are less than $\pm 0.3k_B$. The two corrections are plotted separately in the upper diagram in Fig. 7. The first correction ΔS_1 is only important for very small cluster sizes, and even there it is to a great extent compensated by the second correction ΔS_2, which becomes important for large cluster sizes.

Due to the problems discussed in the Introduction, only few data, both experimental and theoretical are available in the literature—most of them for the isolated vacancy in silicon. For a comparison of our results with reference values

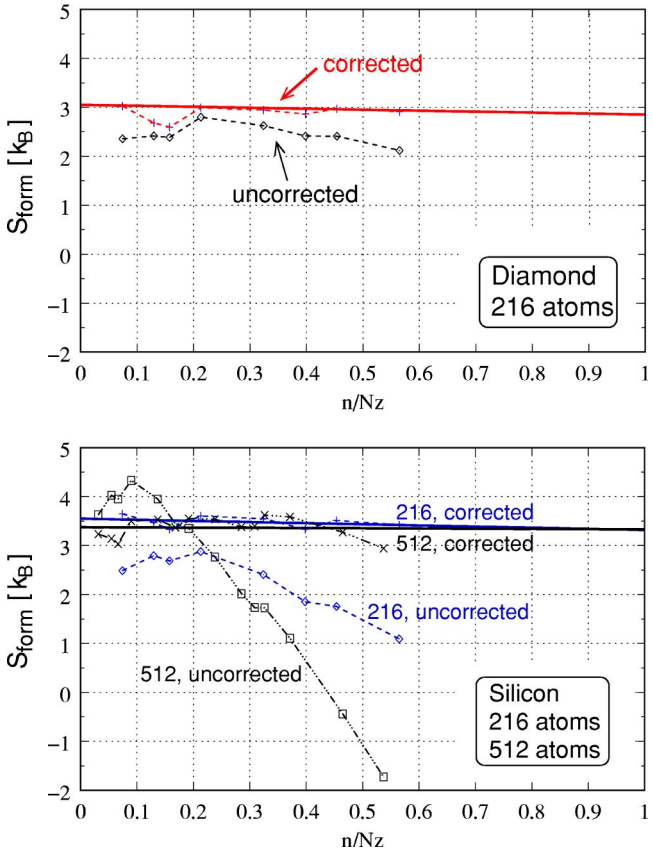

FIG. 6. (Color online) Formation entropy of the vacancy in diamond (upper diagram) calculated in a supercell with $N_Z=216$ atoms and in silicon (lower diagram) calculated in a supercell with $N_Z=216$ atoms (blue, dashed lines) and with $N_Z=512$ atoms (black, dash-dotted lines), restricting the vibrations to N atoms in the shells surrounding the vacancy. The solid lines in both diagrams show linear fits to the corrected data.

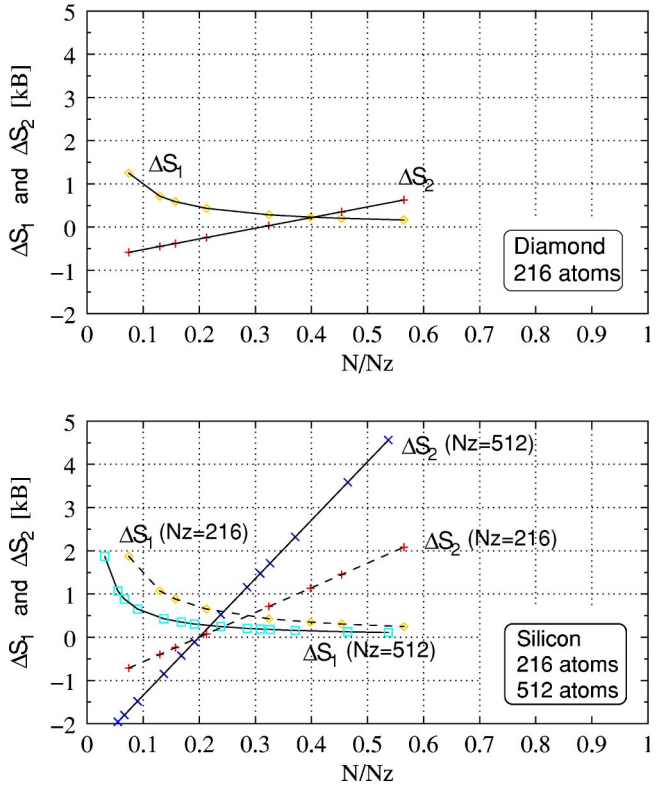

FIG. 7. (Color online) Corrections to the formation entropy for the vacancy in diamond (upper diagram) and silicon (bottom).

we have to perform the same investigations for the vacancy in silicon as for the vacancy in diamond.

In Refs. 3 and 20, the entropy of formation (in the high-temperature approximation) is calculated for the unrelaxed vacancy in silicon, based on a force constant model and including the nearest or next-nearest neighbors of the vacancy only. In Ref. 20 a Green's function technique is used to investigate the influence of the force-constant model on the formation entropy. Although in most simple force-constant models a value of $\approx 1.7k_B$ can be derived for an unrelaxed vacancy in any tetrahedrally bonded material, the results obtained with different methods vary between $1.5k_B$ and up to $8k_B$ and are highly sensitive to the force constants used. For the relaxed vacancy a value of $\approx 3k_B$, as is also obtained by first-principle calculations,[4] is commonly accepted. Small local changes in the force constants can result in large changes in the formation entropy, making a good description of the forces desirable.

The reason for the discrepancies between the formation entropies calculated for the silicon vacancy within different methods is to find in the fact that the vacancy in silicon is one of the most delicate defects with respect to a converged energetical and electronic structure. Even for the less sensitive formation energies convergence starts at supercell sizes larger than 216 atoms, as has been extensively investigated in Refs. 21 and 22. Convergence problems have to be ascribed to the extremely flat potential-energy surface of silicon, which to a high degree influences the quality of the dynamical matrix and, thus, the vibrational frequencies.

Therefore, the calculation of the formation entropy of the vacancy in silicon turns out to be much more complicated than in the case of diamond. Knowing of the convergence problems in silicon, we performed additional calculations in a larger supercell with 512 atoms. For both supercells, the results are plotted in the bottom diagram in Fig. 6. A much stronger divergence compared to the vacancy in diamond is observed here. In the larger supercell with 512 atoms, the diverging behavior of the uncorrected values for the entropy is found to be even worse than in the supercell with 216 atoms. This—at the first view surprising—observation was made by, e.g., Fernández *et al.*, as well.[17] Regarding cluster sizes of $\approx 0.5N_Z$, even negative values occur for S_{form} in the 512 atom cell. Taking a closer look at the corrections derived in the preceding section, these observations can be understood, because the second term of the correction is proportional to $N_Z \Delta V_{\text{core}}$, which is by about one order of magnitude larger for the vacancy in silicon than for the vacancy in diamond (see Table I) and explains the dependence on the supercell size N_Z as well.

The bottom diagram in Fig. 7 shows the two corrections to the formation entropy separately. Again, the first correction ΔS_1 is largely compensated by ΔS_2 for small cluster sizes N. For larger cluster sizes N, correction ΔS_1 is negli-

gible. Here, ΔS_2 is overweighing. In case of diamond, this correction is rather small. However, for the vacancy in silicon, ΔS_2 is of the same order of magnitude as the core entropy itself. A possible reason is the poor convergence behavior caused by the flat potential-energy surface as mentioned above combined with substantially stronger finite size effects.

Nevertheless, with the described corrections, we can obtain a consistent picture even in this case: The total formation entropy of the vacancy in silicon, obtained by extrapolation of the corrected values to $N=N_Z$, results in $3.32k_B$ (216 atoms) and $3.33k_B$ (512 atoms), compare Fig. 6. These values are in good agreement with the reference data discussed above. Variations are slightly larger than in case of diamond, but still in the range of $\pm 0.5k_B$.

E. Migration entropies

The vibrational entropy cannot only be calculated for minimum-energy structures, but also for saddle-point configurations. This enables us to calculate the free energy of activation for migration processes of point defects. The calculation of migration entropies is a much easier task than the calculation of formation entropies, since it does not suffer from the problems discussed in the preceding section. Errors due to artificial constraints by the supercell boundaries or by periodic images can be expected to be of similar magnitude in the compared structures (and thus cancel in ΔS), whereas the comparison of a defective and a perfect supercell as required for the calculation of formation entropies is more sophisticated. The most important quantity to influence the calculated entropies is the accuracy of relaxation of the atoms surrounding the defect, compare, e.g., Ref. 23.

As an example of how the entropy influences migration processes, we discuss the transformation of the isolated silicon vacancy in SiC to the carbon vacancy—carbon antisite ($V_C C_{Si}$) pair.[24,25] Calculations were performed in a 240 atom supercell of 4H-SiC where—for the entropy calculations—all atoms but those on the supercell edges were allowed to vibrate. Differences in calculations including all atoms were found to be in general less than 0.2 eV, most often even less than 0.1 eV, and the same holds for a calculation in a twice as large supercell. Figure 8 shows the structures of the environment of the defect and the energy diagram of the process. Without considering the entropic contributions to this process, the transformation can be activated with 1.7 eV, and the resulting $V_C C_{Si}$ pair is by 1.8 eV more stable than V_{Si} (compare the solid line in Fig. 8) (Ref. 24). By calculating the vibrational spectra of V_{Si}, $V_C C_{Si}$, and the saddle-point structure (obtained as described in Refs. 1 and 24), the entropies of all these structures can be deduced. Using the silicon vacancy as reference, and choosing a common annealing temperature of $T=1800$ K, the free activation energy for the process is obtained (compare the dashed line in Fig. 8). Furthermore, the stabilizing effect of the entropy on the resulting structure can be seen. Both the free-energy barrier and the free energy of the $V_C C_{Si}$ pair are by $\Delta U - T\cdot\Delta S \approx 0.3$ eV lower than the values obtained by calculations at $T=0$ K compared to the silicon vacancy. The free-energy barrier for the $V_{Si} \rightarrow V_C\ C_{Si}$ transformation is, then, 1.4 eV. The $V_C\ C_{Si}$ pair is by 2.1 eV lower in energy than the silicon vacancy. The recombination barrier remains unchanged.

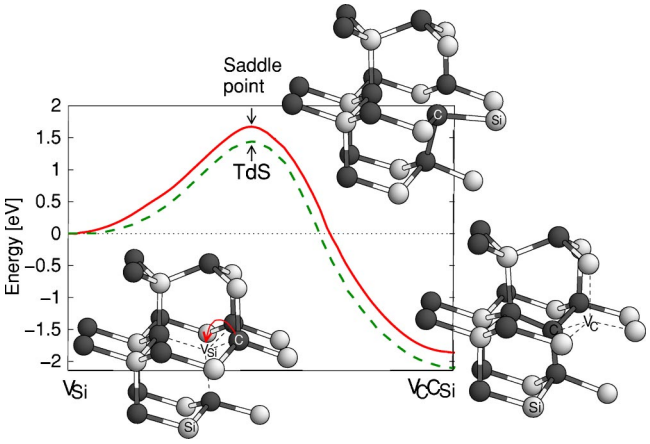

FIG. 8. (Color online) Influence of the vibrational entropy on the transformation of the silicon vacancy into the $V_C\ C_{Si}$ pair. *Solid line*: E_{tot}, *dashed line*: free energy at $T=1800$ K.

As shown in Ref. 1, this process plays a very important role in the mobility and aggregation of antisites. Strong lattice rearrangement during these processes combined with high temperatures needed for their activation, render it important to consider entropic contributions. For a detailed discussion of these topics, the reader is referred to Ref. 1.

IV. CONCLUSION

Summarizing, we have shown the contributions of vibrational entropy to be important in many cases, i.e., when the investigated process runs at elevated temperatures or when strong lattice rearrangements occur during the process. Furthermore, we have proposed a way to calculate the entropy of formation by addressing the problems of finite-size effects arising if using common supercell approaches. These difficulties can, though, be overcome with the help of linear elasticity theory, as we have demonstrated at the example of isolated vacancies in diamond and silicon. A good agreement of the values obtained like this with reference data has been found. With minor changes, the equations given in this paper can as well be applied to other defect structures, as, e.g., interstitials. The treatment of dopant atoms requires further consideration, since the chemical potentials of the respective dopant materials have to be included. Due to error cancellation, the calculation of the entropy of migration does not suffer from these problems and has been shown to be of non-negligible order of magnitude in high-temperature processes.

ACKNOWLEDGMENTS

The author wishes to thank Prof. P. Deák for giving an impulse to these investigations and Dr. U. Gerstmann for fruitful discussions.

APPENDIX

In linear elasticity theory, the strained material is described by a displacement field

$$\mathbf{u}(\mathbf{r}) = \mathbf{r}' - \mathbf{r}, \tag{A1}$$

where $\mathbf{r}$ are the positions of the atoms in the unstrained $\mathbf{r}'$ in the strained lattice. From this displacement field, the components of the strain tensor ε_{ij} are obtained as

$$\varepsilon_{ij} = \frac{1}{2}\left(\frac{\partial u_i}{\partial x_j} + \frac{\partial u_j}{\partial x_i}\right). \tag{A2}$$

The diagonal elements ε_{ii} define the volume change due to defect relaxation, the so-called dilatation

$$\delta = \frac{\delta V}{V} = \varepsilon_{11} + \varepsilon_{22} + \varepsilon_{33}. \tag{A3}$$

We consider a spherical isotropic continuum of radius R. For a point defect with spherical symmetry, as can be assumed in good approximation for the vacancy, only radial strain occurs, and so we obtain

$$\nabla^2 \delta = 0 \qquad \text{with} \qquad \delta = \delta(r), \tag{A4}$$

for the dilatation δ. Since $\delta = \boldsymbol{\nabla} \cdot \mathbf{u}$, the displacement field has to be of the form

$$\mathbf{u}(\mathbf{r}) = \left(\frac{A}{r^3} + B\right) \cdot \mathbf{r}, \tag{A5}$$

with constants A and B to be determined by the boundary conditions.

Expressions for the radial strain $\varepsilon_{\mathrm{rr}}$ and the dilatation δ follow from Eq. (A5):

$$\varepsilon_{\mathrm{rr}} = -\frac{2A}{r^3} + B, \qquad \delta = \boldsymbol{\nabla} \cdot \mathbf{u} = 3B. \tag{A6}$$

Via Hooke's law and using the Lamé constants λ and μ, the stress tensor

$$\sigma_{ij} = 2\mu\varepsilon_{ij} + \lambda\delta\delta_{ij} \tag{A7}$$

can be calculated from the strain tensor ε. With this relation and the boundary condition that no stress is left at the surface of the sphere with $r = R$ (cf. Figs. 4 and 5), the constant B can be expressed in terms of A:

$$\sigma_{\mathrm{rr}}(r = R) = 0$$

$$\Leftrightarrow 2\mu\varepsilon_{\mathrm{rr}} + \lambda\delta = 0$$

$$\Leftrightarrow B = \frac{4\mu}{2\mu + 3\lambda}\frac{A}{R^3}. \tag{A8}$$

The displacement field $\mathbf{u}$ becomes then

$$\mathbf{u}(\mathbf{r}) = A\left(\frac{1}{r^3} + \frac{4\mu}{2\mu + 3\lambda}\frac{1}{R^3}\right) \cdot \mathbf{r} = \mathbf{u}_s(\mathbf{r}) + \mathbf{u}_d(\mathbf{r}), \tag{A9}$$

with a shear term $\mathbf{u}_s$ and a dilatation term $\mathbf{u}_d$.[5]

Let the displacement at the radius r_{core} of the defect core be $u(r_{\mathrm{core}}) = \eta r_{\mathrm{core}}$, then A can be written as

$$A = \frac{1}{1 + \dfrac{4\mu r_{\mathrm{core}}^3}{(2\mu + 3\lambda)R^3}}\eta r_{\mathrm{core}}^3 \underset{\frac{r_{\mathrm{core}}}{R} \ll 1}{\approx} \eta r_{\mathrm{core}}^3. \tag{A10}$$

Now it can be seen that the dilatation

$$\delta = 3B = \frac{12\mu\eta r_{\mathrm{core}}^3}{(2\mu + 3\lambda)R^3} \tag{A11}$$

tends to zero for an *infinite* crystal, but this is not true for a *finite* crystal, and especially not for the from the macroscopic view small supercells.

At the surface of the outer sphere ($r = R$), the shear part of Eq. (A9) causes the volume change

$$\Delta V_s = 4\pi R^2 \cdot u_s(R) = 4\pi\eta r_{\mathrm{core}}^3, \tag{A12}$$

i.e., the volume change the defect would cause in an infinitely extended crystal. The dilatation term yields

$$\Delta V_d = 4\pi R^2 \cdot u_d(R) = 4\pi\frac{4\mu}{2\mu + 3\lambda}\eta r_{\mathrm{core}}^3. \tag{A13}$$

Using instead of the Lamé constants μ and λ the poisson ratio

$$\nu = \frac{\lambda}{2(\lambda + \mu)}, \tag{A14}$$

we get

$$\Delta V_d = 4\pi\frac{2(1 - 2\nu)}{1 + \nu}\eta r_{\mathrm{core}}^3, \tag{A15}$$

for the dilatation part and thus the total volume change becomes

$$\Delta V_{\mathrm{tot}} = 4\pi\frac{3(1 - \nu)}{1 + \nu}\eta r_{\mathrm{core}}^3. \tag{A16}$$

The dilatation part arises only due to image forces at the surface of the sphere. From Eqs. (A15) and (A16) it follows that

$$\frac{\Delta V_d}{\Delta V_{\mathrm{tot}}} = \frac{2}{3}\left(\frac{1 - 2\nu}{1 - \nu}\right). \tag{A17}$$

This sets the volume change due to image forces (which is needed for the entropy correction) in relation to the total volume change.[5]

*Email: address: rauls@phys.upb.de

[1] E. Rauls, Th. Frauenheim, A. Gali, and P. Deák, Phys. Rev. B **68**, 155208 (2003).
[2] Th. Frauenheim, G. Seifert, M. Elstner, Z. Hajnal, G. Jungnickel, D. Porezag, S. Suhai, and R. Scholz, Phys. Status Solidi B **217**, 41 (2000).
[3] M. Lannoo and J.C. Bourgoin, Solid State Commun. **32**, 913 (1979).
[4] M. Scheffler and J. Dabrowski, Philos. Mag. A **58**, 107 (1988).
[5] C.P. Flynn, *Point Defects and Diffusion* (Clarendon Press, Oxford, 1972).
[6] Ch. Kittel, in *Physik der Wärme*, edited by R. Oldenbourg (Springer-Verlag, New York, 1973).
[7] R. LeSar, R. Najafabadi, and D.J. Srolovitz, Phys. Rev. Lett. **63**, 624 (1989).
[8] A.P. Sutton, Philos. Mag. A **60**, 147 (1989).
[9] Y. Mishin, M.R. Sorensen, and A.F. Voter, Philos. Mag. A **81**, 2591 (2001).
[10] R. Jones, Philos. Trans. R. Soc. London, Ser. A **341**, 351 (1992).
[11] M. Bockstedte, A. Kley, J. Neugebauer, and M. Scheffler, Comput. Phys. Commun. **107**, 187 (1997).
[12] H. Kuchling, *Taschenbuch der Physik* (1986).
[13] A. Gali (private communication).
[14] A. Mattausch (private communication).
[15] M.R. Jarvis, I.D. White, R.W. Godby, and M.C. Payne, Phys. Rev. B **56**, 14 972 (1997).
[16] J.D. Cox, D.D. Wagman, and V.A. Medvedev, *CODATA Key Values for Thermodynamics* (Hemisphere, New York, 1989).
[17] J.R. Fernández, A.M. Monti, and R.C. Pasianot, Phys. Status Solidi B **219**, 245 (2000).
[18] R.D. Hatcher, R. Zeller, and P.H. Dederichs, Phys. Rev. B **19**, 5083 (1979).
[19] L.D. Landau and E.M. Lifschitz, *Lehrbuch der Theoretischen Physik, Band VII, Elastizitätstheorie* (Akademie-Verlag, Berlin, 1975).
[20] M. Lannoo and G. Allan, Phys. Rev. B **25**, 4089 (1982).
[21] U. Gerstmann, E. Rauls, H. Overhof, and Th. Frauenheim, Phys. Rev. B **65**, 195201 (2002).
[22] M.J. Puska, S. Pöykkö, M. Pesola, and R.M. Nieminen, Phys. Rev. B **58**, 1318 (1998).
[23] D. Morgan, A. van de Walle, G. Ceder, J.D. Althoff, and D. de Fontaine, Modell. Simul. Mater. Sci. Eng. **8**, 295 (2000).
[24] E. Rauls, Th. Lingner, Z. Hajnal, S. Greulich–Weber, Th. Frauenheim, and J.-M. Spaeth, Phys. Status Solidi B **217/2**, R1 (2000).
[25] Th. Lingner, S. Greulich-Weber, J.M. Spaeth, U. Gerstmann, E. Rauls, Z. Hajnal, Th. Frauenheim, and H. Overhof, Phys. Rev. B **64**, 245212 (2001).